Q-band Electron Nuclear Double Resonance of Ferric Bleomycin and Activated Bleomycin Complexes with DNA: Fe(III) Hyperfine Interaction with ^{31}P and DNA-Induced Perturbation to Bleomycin Structure

Andrei Veselov,[†] Richard M. Burger,[‡] and Charles P. Scholes*[,†]

Contribution from the Department of Chemistry, University at Albany, State University of New York, Albany, New York 12222, and Laboratory of Chromosome Biology, Public Health Research Institute, 455 First Avenue, New York, New York 10016

Received June 27, 1997. Revised Manuscript Received November 11, 1997

Abstract: Q-band electron nuclear double resonance (ENDOR) has measured anisotropic, distance-dependent dipolar hyperfine couplings from iron in ferric bleomycin [Fe(III)-BLM] and in activated bleomycin [Act-BLM] to ^{31}P of substrate DNA. Studies were focused on bleomycin complexes with a self-complementary duplex DNA 10-mer, d(GGAAGCTTCC)$_2$, containing a 5′-G-C-3′ sequence that is selective for bleomycin cleavage (Mao, Q.; Fulmer, P.; Li, W.; DeRose, E. G.; Petering, D. H. *J. Biol. Chem.* **1996**, *271*, 6185−6191). Bleomycin complexes with high molecular weight calf thymus DNA were also used. Fe(III)-BLM and Act-BLM complexes with the 10-mer and the calf thymus DNA showed anisotropic ^{31}P dipolar hyperfine couplings from which an Fe(III)-to-^{31}P distance was estimated at 7.4 ± 0.2 Å. High-resolution, angle-selected ENDOR of the Fe(III)-BLM 10-mer complex showed that the Fe(III)-to-^{31}P vector lay at 25 ± 5° to the maximal g value direction, where the latter direction pointed near the exchangeable protons on axial BLM ligands and is associated with the maximal hyperfine couplings of these protons (Veselov, A.; Sun, H.; Sienkiewicz, A.; Taylor, H.; Burger, R. M.; Scholes, C. P. *J. Am. Chem. Soc.* **1995**, *117*, 7508−7512). Proton ENDOR features of the Fe(III)-BLM but not Act-BLM were perturbed by DNA substrate. In the presence of the 10-mer and the calf thymus DNA, proton ENDOR revealed distinct perturbation to the frequencies of three sets of nonexchangeable protons assigned to the BLM macrocycle and estimated to be 2.9−3.5 Å from Fe(III) and to the frequencies of exchangeable, axially located protons. In contrast, the hyperfine couplings of covalently bonded, first-shell nitrogen and [^{17}O]peroxy ligands were unchanged.

Introduction

The chemotherapeutic activity of bleomycin, a glycopeptide antibiotic, derives from its ability to induce DNA strand scission.[1] Bleomycins bind and degrade duplex DNA in the presence of Fe(II), O_2, and a reductant. When ferrous bleomycin [Fe(II)-BLM] is exposed to O_2, a transient activated form of bleomycin (Act-BLM) appears which is kinetically competent to initiate DNA cleavage[2] through a reaction pathway that is thought to involve free radical intermediates.[1b,c] Recent studies strongly suggest that Act-BLM is a ferric hydroperoxide, formally HOO−Fe(III)-BLM;[3a] this is the last detectable intermediate prior to DNA strand scission.[1c] An oxygen kinetic isotope effect indicates that O−O bond cleavage is rate limiting in the breakdown of Act-BLM.[3b] Act-BLM and its final product, ferric bleomycin [Fe(III)-BLM], are low-spin ferric complexes. Act-BLM has g values of g_{max}, g_{inter}, g_{min} = 2.26, 2.17, 1.94,[2d] and Fe(III)-BLM has g values of g_{max}, g_{inter}, g_{min} = 2.45, 2.18, 1.89.[2a,d] The structural basis for bleomycin action requires knowledge of the nature of the BLM−oligonucleotide complex. Fe(III)-BLM or Act-BLM, either by themselves or as oligonucleotide complexes, have yet to be crystallized. Biologically active Act-BLM and Fe(III)-BLM forms are unsuitable for multidimensional structural NMR study because the ferric ion is a strong relaxer and because Act-BLM is not stable under ambient experimental conditions. Furthermore, their complexes, if with higher molecular weight DNA, have unsuitably broad NMR features. High-resolution NMR of BLM initially focused on nonparamagnetic Zn-BLM[4a] and CO−Fe(II)-BLM[4b] and more recently on the stable, nonparamagnetic HOO−Co(III)-BLM[4c−h] analogue of Act-BLM. From the latter Co(III) system the conformation of the BLM−oligonucleotide complex and the potential basis for the 5′-G-pyrimidine-3′ sequence selectivity of BLM cleavage were elucidated.[4f,g]

* To whom correspondence should be addressed.
[†] University at Albany, State University of New York.
[‡] Public Health Research Institute.

(1) (a) Takeshita, M.; Grollman, A. P. In *Bleomycin: Chemical, Biochemical, and Biological Aspects*; Hecht, S. M., Ed.; Springer-Verlag: New York; 1979; pp 207−221. (b) Stubbe, J.; Kozarich, J. W. *Chem. Rev.* **1987**, 87, 1107−1136. (c) Stubbe, J.; Kozarich, J. W.; Wu, W.; Vanderwall, D. *Acc. Chem. Res.* **1996**, *29*, 322−330.

(2) (a) Burger, R. M.; Peisach, J.; Blumberg, W. E.; Horwitz, S. B. *J. Biol. Chem.* **1979**, 254, 10906−10912. (b) Burger, R. M.; Horwitz, S. B.; Peisach, J.; Wittenberg, J. B. *J. Biol. Chem.* **1979**, 254, 12299−12302. (c) Burger, R. M.; Adler, A. D.; Horwitz, S. B.; Mims, W. B.; Peisach, J. *Biochemistry* **1981**, *20*, 1701−1704. (d) Burger, R. M.; Peisach, J.; Horwitz, S. B. *J. Biol. Chem.* **1981**, 256, 11636−11644. (e) Burger, R. M.; Kent, T. A.; Horwitz, S. B.; Münck, E.; Peisach, J. *J. Biol. Chem.* **1983**, 258, 1559−1564. (f) Burger, R. M.; Blanchard, J. S.; Horwitz, S. B.; Peisach, J. *J. Biol. Chem.* **1985**, 260, 15406−15409. (g) Kuramochi, H.; Takahashi, K.; Takita, T.; Umezawa, H. *J. Antibiot. (Tokyo)* **1981**, 34, 578−582.

(3) (a) Sam, J. W.; Tang, X.-J.; Peisach, J. *J. Am. Chem. Soc.* **1994**, *116*, 5250−5256. (b) Burger, R. M.; Tian, G.; Drlica, K. J. *Am. Chem. Soc.* **1995**, 117, 1167−1168.

S0002-7863(97)02138-0 CCC: $15.00
Published on Web 01/22/1998

Cryogenic electron nuclear double resonance (ENDOR) of paramagnetic Act-BLM and Fe(III)-BLM has provided evidence for electron spin delocalization not attainable by NMR, notably hyperfine couplings to a ^{17}O-containing ligand of Act-BLM derived from $^{17}O_2$ and to first-shell ^{14}N ligands having isotropic couplings.[5a] ENDOR further revealed strongly coupled exchangeable protons of Act-BLM and Fe(III)-BLM that are attached to immediate nitrogen or oxygen axial ligands.[5a] ENDOR studies are here extended to probe the interaction of Act-BLM and Fe(III)-BLM with DNA substrates, primarily in the form of a low molecular weight oligonucleotide 10-mer, d(GGAAGCTTCC)$_2$, having a known internal BLM cleavage site[4e] and also in the form of generic calf thymus (CfT-DNA). A recently reported EPR study of Fe(III)-BLM and other paramagnetic metal-BLM forms has indicated perturbation of the metal-binding domain by this 10-mer.[4h] The present studies show proximity of the iron to the [^{31}P]phosphate of the DNA substrate and perturbation to the BLM structure, specifically as evidenced by proton ENDOR.

Experimental Section

Our Q-band (34.0 GHz) ENDOR system has been previously described.[5] BLM was obtained from Bristol Myers. The self-complementary oligonucleotide 10-mer d(GGAAGCTTCC) purified with research grade HPLC was purchased from Oligos Etc. Inc., Wilsonville, OR, and calf thymus DNA was obtained from Sigma. All samples contained 20 mM Na−Hepes buffer, pH 7.8 (or its counterpart, lyophilized and reconstituted with D_2O), and 50% (v/v) ethylene glycol (perdeuterated for D_2O-containing samples). All constituents were dissolved in H_2O or D_2O, as appropriate. Exchangeable protons were eliminated by sample preparation in 99.9% D_2O and 99% perdeuterated ethylene glycol (MSD Isotopes). Oligonucleotides were dissolved in buffer, annealed by heating to 75 °C (predicted mp 38.6 °C), and cooled slowly. DNA from calf thymus (Sigma) was dissolved in buffer with gentle shaking for several days, sheared in a French press, and then redissolved at 0.1 M nucleic acid bases after ethanol precipitation. For Fe(III)-BLM samples, ferric ammonium sulfate solution was added to a slight excess of BLM, followed by buffer, CfT-DNA or oligodeoxynucleotides as needed, and ethylene glycol. Samples were then frozen in 2.0 mm inside diameter, 2.4 mm outside diameter quartz EPR tubes in liquid nitrogen. Fe(III)-BLM samples contained 2.5 mM BLM, 2.0 mM Fe(III), and no DNA; 1.6 mM BLM, 1.4 mM Fe(III), and 1.6 mM d(GGAAGCTTCC)$_2$; or 0.5 mM BLM, 0.4 mM Fe(III), and 10 mM DNA (nucleic acid bases). For Act-BLM, buffered BLM solutions were equilibrated with either $^{16}O_2$ or $^{17}O_2$ and chilled to 4 °C, followed by small volume additions, with mixing, of (2 μL each per 100 μL sample) NADH (in buffer), ferrous ammonium sulfate, and phenazine methosulfate. CfT-DNA or oligodeoxynucleotides were then added as needed, followed by ethylene glycol and freezing in liquid nitrogen about a minute after Fe(II) addition. Some $^{16}O_2$ samples contained D_2O. Act-BLM samples contained 0.25 mM BLM, 0.2 mM Fe(II), and no DNA; 0.6 mM BLM, 0.5 mM Fe(II), and 0.7 mM d(GGAAGCTTCC)$_2$ with $^{16}O_2$ or 1.4 mM d(GGAAGCTTCC)$_2$ with $^{17}O_2$; or 0.5 mM BLM, 0.4 mM Fe(II), and 10 mM CfT-DNA. Because the concentration of Act-BLM depends on the available concentration of O_2, the concentrations of Act-BLM used in these studies were less than half those of Fe(III)-BLM, and so signals tended to be smaller from Act-BLM. For detailed angle-selected ENDOR spectra, the high-concentration sample of Fe(III)-BLM complexes with 10-mer provided the greatest sensitivity. The EPR spectra of Fe(III)-BLM and Act-BLM were as reported initially by Burger,[2a,d] and as in ref 5a, rapid passage Act-BLM EPR spectra showed negligible contamination with Fe(III)-BLM.

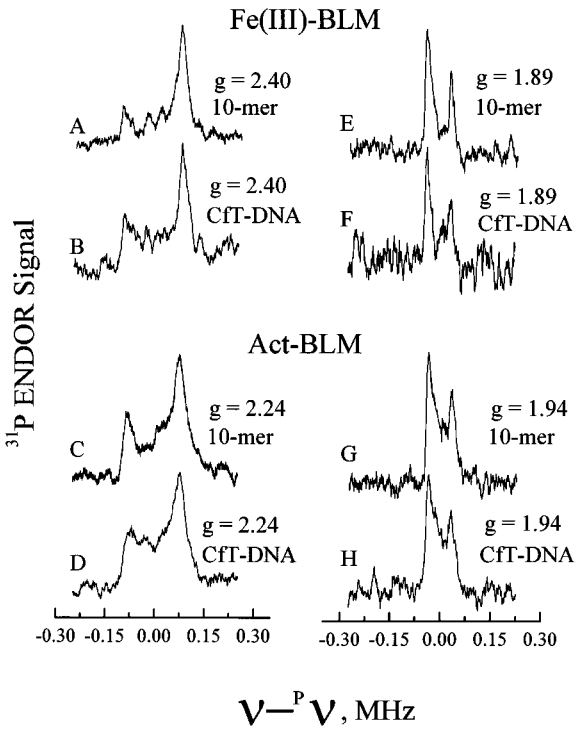

Figure 1. ^{31}P ENDOR spectra centered at the appropriate $^{P}\nu_{NMR}$. Each spectrum was obtained under adiabatic rapid passage conditions (χ') with small ~0.15 G, 100 kHz field modulation, ~1 μW microwave power, and ~20 W RF (radio frequency) power, at a frequency sweep rate of 0.1 MHz/s and with approximately 20 min of data collection and an experimental time constant of 0.08 s. Samples (A) Fe(III)-BLM + 10-mer, $g = 2.40$, $H = 1.014$ T; (B) Fe(III)-BLM + CfT-DNA, $g = 2.40$, $H = 1.014$ T; (C) Act-BLM + 10-mer, $g = 2.24$, $H = 1.084$ T; (D) Act-BLM + CfT-DNA, $g_{max} = 2.24$, $H = 1.084$ T; (E) Fe(III)-BLM + 10-mer, $g = 1.89$, $H = 1.284$ T; (F) Fe(III)-BLM + CfT-DNA, $g = 1.89$, $H = 1.284$ T; (G) Act-BLM + 10-mer, $g = 1.94$, $H = 1.254$ T; (H) Act-BLM + CfT-DNA, $g = 1.94$, $H = 1.254$ T.

Results and Discussion

^{31}P ENDOR Reflecting the BLM−DNA Interaction. Hyperfine coupled spin 1/2 nuclei like ^{31}P or ^{1}H have first-order ENDOR frequencies, $\nu_{ENDOR} = |\nu_{NMR} \pm A/2|$, where ν_{NMR} is the free nuclear NMR frequency (for ^{31}P, $^{P}\nu_{NMR} = 20.7$ MHz at 1.2 T, and for ^{1}H, $^{H}\nu_{NMR} = 51.1$ MHz at 1.2 T) and A is the hyperfine coupling. Figure 1 presents ^{31}P ENDOR spectra, centered at $^{P}\nu_{NMR}$, which were recorded close to extremal g values (g_{max} and g_{min}) where single-crystal-like ENDOR spectra are typically obtained. Spectra of Figure 1A,B,E,F were from Fe(III)-BLM, and spectra of Figure 1C,D,G,H were from Act-BLM. Spectra A, C, E, and G were obtained in the presence of 10-mer and spectra B, D, F, and H in the presence of CfT-DNA. The ENDOR signals with well-resolved outlying splittings distinctly arose from a unique ^{31}P for which at g_{max} the hyperfine splitting (0.18 ± 0.01 MHz for Fe(III)-BLM and 0.16 ± 0.01 MHz for Act-BLM) was more than twice the size of

(4) (a) Manderville, R. A.; Ellena, J. F.; Hecht, S. M. *J. Am. Chem. Soc.* **1994**, *116*, 10851−10852. (b) Akkerman, M. A. J.; Neijman, E. W. J. F.; Wijmenga, S. S.; Hilbers, C. W.; Bermel., W. *J. Am. Chem. Soc.* **1990**, *112*, 7462−7474. (c) Xu, R. X.; Nettesheim, D.; Otvos, J. D.; Petering, D. H. *Biochemistry* **1994**, *33*, 907−916. (d) Wu., W.; Vanderwall, D. E.; Stubbe, J.; Kozarich, J. W.; Turner, C. J. *J. Am. Chem. Soc.* **1994**, *116*, 10843−10844. (e) Mao, Q.; Fulmer, P.; Li, W.; DeRose, E. F.; Petering, D. H. *J. Biol. Chem.* **1996**, 271, 6185−6191. (f) Wu., W.; Vanderwall, D. E.; Lui, S. M.; Tang, X.-J.; Turner, C. J.; Kozarich, J. W.; Stubbe, J. *J. Am. Chem. Soc.* **1996**, *118*, 1268−1280. (g) Wu., W.; Vanderwall, D. E.; Turner, C. J.; Kozarich, J. W.; Stubbe, J. *J. Am. Chem. Soc.* **1996**, *118*, 1281−1294. (h) Fulmer, P.; Zhao, C.; Li, W.; DeRose, E.; Antholine, W. E.; Petering, D. H. *Biochemistry* **1997**, *36*, 4367−4374.

(5) (a) Veselov, A.; Sun, H.; Sienkiewicz, A.; Taylor, H.; Burger, R. M.; Scholes, C. P. *J. Am. Chem. Soc.* **1995**, *117*, 7508−7512. (b) Sienkiewicz, A.; Smith, B. G.; Veselov, A.; Scholes, C. P. *Rev. Sci. Instrum.* **1996**, 67, 2134−2138.

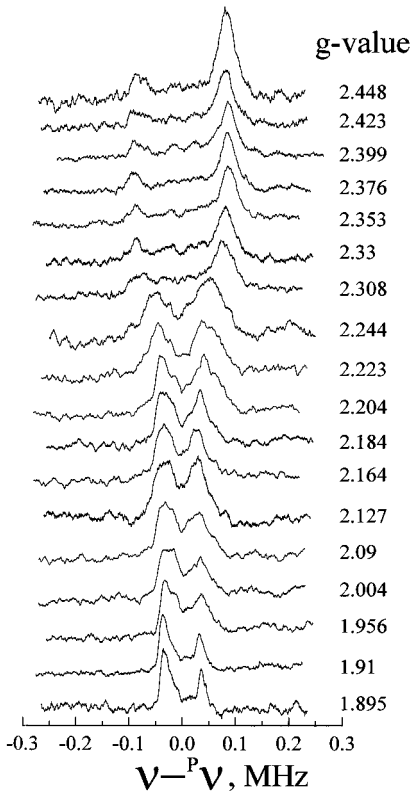

Figure 2. Experimental variation of ^{31}P ENDOR features from Fe(III)-BLM in the presence of 10-mer presented from a maximum $g = 2.448$ to a minimum $g = 1.895$. The experimental conditions for obtaining ^{31}P spectra were as in Figure 1.

the splitting near g_{min} (0.07 ± 0.01 MHz for both). This marked anisotropy in ENDOR splittings between g_{max} and g_{min} is strong evidence for an anisotropic hyperfine tensor. Figure 2 presents a compendium of experimental ^{31}P ENDOR spectra from the Fe(III)-BLM−10-mer complex which varied systematically in their splittings with g values from g_{max} to g_{min}. Such variation of ENDOR frequencies was simulated by angle-selected ENDOR theory,[7a−c] whose input parameters were the elements of the anisotropic hyperfine tensor and angle(s) describing the relative angular orientation of the hyperfine and g tensors. We provide a comparison in Figure 3 of the well-resolved outlying experimental ^{31}P ENDOR splittings from the Fe(III)-BLM−10-mer complex with the predicted outlying splittings from angle-selected ENDOR simulations. These simulations were based on an anisotropic tensor having $A_z, A_y, A_x = 0.19, -0.086, -0.075$ MHz. All elements of this hyperfine tensor were explained by dipolar coupling[8] of ^{31}P to an Fe(III) that has an

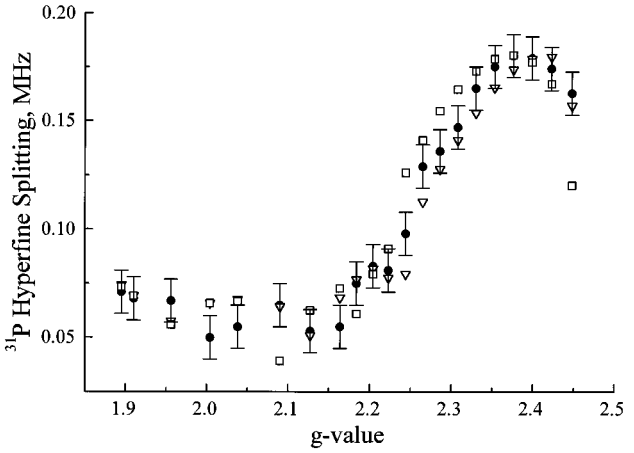

Figure 3. A comparison of ^{31}P splittings, experimentally observed by ENDOR of Fe(III)-BLM over a range of g values from $g = 2.448$ to $g = 1.895$ (solid circles with error bars), corresponding to computed, angle-selected simulations arising from an anisotropic hyperfine tensor having $A_z, A_y, A_z = 0.19, -0.086, -0.075$ MHz. The A_z, A_y components of the tensor were rotated in the $g_{max}-g_{inter}$ plane; the results of making such tensor rotations with respect to the g_{max} direction by either 20° (open triangles) or 30° (open squares) are shown.

anisotropic g tensor, $g_{max}, g_{inter}, g_{min} = 2.45, 2.18, 1.89$, and a distance $\mathbf{R} = 7.4 \pm 0.2$ Å from ^{31}P to Fe(III). The simulations leading to Figure 3 predicted outlying hyperfine splittings which were maximal near g_{max} and minimal over the large range of g values between g_{inter} and g_{min}. An improved fit of angle-selected splittings to the data of Figure 3 was found when the A_z and A_y axes were subsequently rotated in the $g_{max}-g_{inter}$ plane away from the g_{max} and g_{inter} directions. As a function of the rotation angle of A_z and A_y with respect to g_{max}, these simulations predicted splittings that were, like those experimentally measured, largest near but not precisely at g_{max}. As a result, the vector $\mathbf{R}$ was predicted to make an angle of $25 \pm 5°$ in the $g_{max}-g_{inter}$ plane with respect to the g_{max} direction. The angle-selected theory can be used to predict overall ENDOR spectra,[9] and we compare our overall computed spectra to experimental spectra in Figure S-1 in the Supporting Information. For ^{31}P ENDOR spectra at the respective g_{max} and at the respective g_{min} (Figure 1), the small differences in dipolar hyperfine splitting between Fe(III)-BLM and Act-BLM were well explained by the slightly different electronic g values of the two complexes; the implication is that the ^{31}P−Fe(III) distances are identical in the DNA substrate complexes of Fe(III)-BLM and Act-BLM.

Proton ENDOR Reflecting the BLM−DNA Interaction. The interaction with 10-mer and calf thymus DNA substrates led to new or altered ENDOR-detectable proton features from

(6) Positive ENDOR results definitively showed a maximal ~0.17 MHz nuclear hyperfine coupling to ^{31}P from our samples. We have sought without success for ^{31}P ENDOR features with couplings >0.17 MHz. We point out that a lack of ENDOR results, which might be due to inappropriate spin relaxation or misorientation broadening, does not so definitively rule out larger couplings to other ^{31}P nuclei. NMR-derived coordinates from the possibly related Zn-BLM−d(CGCTAGCG)$_2$ (ref 4a) indicated a 7.2 Å distance from the BLM metal to the G_6-C_7 phosphate but also indicated a 5.7 Å distance to the C_7-G_8 phosphate. The latter metal−^{31}P distance, if valid for our iron complexes, might well produce a larger dipolar coupling than 0.17 MHz.

(7) (a) Hoffman, B. M.; Martinsen, J.; Venters, R. A. *J. Magn. Reson.* **1984**, 59, 110−123. (b) Hoffman, B. M.; Venters, R. A.; Martinsen, J. *J. Magn. Reson.* **1985**, 62, 537−542. (c) Hoffman, B. M.; DeRose, V. J.; Doan, P. E.; Gurbiel, R. J.; Houseman, A. L. P.; Telser, J. In *Biological Magnetic Resonance, Vol. 13: EMR of Paramagnetic Molecules*; Berliner, L. J., Reuben, J., Eds.; Plenum Press: New York, 1993. (d) Fann, Y.-C.; Ong, J.-L.; Nocek, J. M.; Hoffman, B. M. *J. Am. Chem. Soc.* **1995**, *117*, 6109−6116.

(8) The point dipole interaction between a nuclear spin $\mathbf{I}$ and electron spin $\mathbf{S}$ separated by a distance $\mathbf{R}$ is $A_D = \{1/hR^3\}(3(\mu_S\cdot\mathbf{R})(\mu_I\cdot\mathbf{R})/R^2 - \mu_S\cdot\mu_I)$. The nuclear magnetic moment is $\mu_I = g_n\beta_n(I_x + I_y + I_z)$, and the electron magnetic moment in the g tensor principal axis system is $\mu_S = \beta_e(g_xS_x + g_yS_y + g_zS_z)$. g_n is the nuclear g value (=2.261 for ^{31}P and 5.585 for ^{1}H); β_n and β_e are the nuclear and electron Bohr magnetons. Such a general expression allows the dipolar tensor to be modified by electron g anisotropy and by rotation of the direction of $\mathbf{R}$ with respect to the g tensor principal axes.

(9) Angle-selected ENDOR frequencies are readily computed. A significant result of the anisotropic dipole tensor is that there are ENDOR transitions and intensity with very small splittings close to $^P\nu_{NMR}$ at intermediate g values. ENDOR features near g_{max} tend to show splitting or broadening if the hyperfine tensor is not collinear with the g tensor, and the maximum hyperfine splitting does not occur at g_{max}. Because the ENDOR phenomenon depends on numerous coupled spin relaxation processes, our experience is that detailed line shape and intensity agreement between computed ENDOR spectra and experimentally measured ENDOR spectra will be qualitative. ENDOR peak frequency information, as opposed to line shape and intensity information, is the ENDOR information.

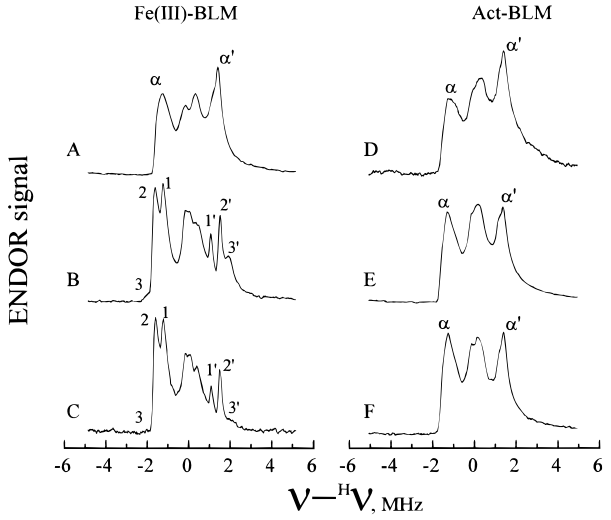

Figure 4. Proton ENDOR carried out to show the effect of DNA substrate perturbation on nonexchangeable proton features of Fe(III)-BLM and Act-BLM as collected at their respective values of g_{min} in deuterated solvent. Each spectrum was obtained under adiabatic rapid passage conditions (χ') with 1.0 G, 100 Hz field modulation, ~1 μW microwave power, and ~20 W RF power, at a frequency sweep rate of 2 MHz/s and with approximately 5 min of data collection and an experimental time constant of 0.04 s. Parts A−C were from Fe(III)-BLM as obtained at $g = 1.89$ and $H = 1.284$ T: (A) without DNA; (B) plus 10-mer; (C) plus CfT-DNA. Parts D−F were obtained from Act-BLM at $g = 1.94$ and $H = 1.254$ T: (D) without DNA; (E) plus 10-mer; (F) plus CfT-DNA.

Fe(III)-BLM, but not Act-BLM. These features were especially obvious from nonexchangeable protons assigned (below) to the BLM macrocycle (Figure 4B,C with DNA substrates compared to Figure 4A without DNA). Exchangeable protons of Fe(III)-BLM assigned to axial ligands[5a] also had their ENDOR frequencies perturbed by the presence of 10-mer (see Figure S-2 in the Supporting Information). These differences in proton ENDOR spectra appeared to reflect improved resolution, the result of a better defined Fe(III)-BLM structure in the presence of 10-mer and CfT-DNA. However, the immediate first-shell metal−ligand hyperfine structure from ^{14}N of Act-BLM and Fe(III)-BLM and [^{17}O]peroxy of Act-BLM remained unchanged in the presence of 10-mer as shown in the Supporting Information, Figure S-3.

Nonexchangeable proton features in Figure 4B,C (arbitrarily labeled 1,1′, 2,2′, and 3,3′ and having respective splittings of 2.3, 3.4, and 4.0 MHz) appeared at g_{min} from Fe(III)-BLM in the presence of either 10-mer or CfT-DNA. These proton features had splittings in the same general range as the broader unresolved features α,α′ of Fe(III)-BLM in the absence of DNA substrate or of Act-BLM in the presence or absence of DNA. Although the orientation of these nonexchangeable protons with respect to the g_{min} direction is not certain, their 2.3−4.0 MHz hyperfine couplings translated into metal−proton distances in the 2.9−3.5 Å range. A metal−proton distance in the 2.9−3.3 Å range was estimated for the nonexchangeable protons on the C(2) of the β-hydroxy histidine, on α and β carbons of β-hydroxyhistidine, and on the β-carbon of aminoalanine in the related Zn-BLM−d(CGCTAGCG)$_2$.[4c] There appears to be the potential for configurational flexibility of these parts of the BLM macrocycle, and it may be that binding to DNA substrate stabilizes a conformation. Similarly the conformation of axial ligand protons, particularly if they are exchangeable protons on the primary amine ligand provided by the β-aminoalanine moiety,[4f,g] may be stabilized by interaction of DNA substrate with the BLM macrocycle.

The Act-BLM features at g_{min} that correspond to those shown for Fe(III)-BLM are provided in Figure 4D−F, and there was virtually no difference between these Act-BLM spectra in the presence (Figure 4E,F) or the absence (Figure 4D) of DNA. Since the OOH−Co(III)-BLM analogue of Act-BLM reportedly has a highly specific hydrogen-bonding interaction of its metal binding domain and of its hydroperoxide to oligonucleotides[4f,g] like our 10-mer, we were surprised that Fe(III)-BLM, rather than the Act-BLM, had better resolution of its proton features when complexed with DNA substrates. An explanation for the lack of ENDOR-resolved structural changes with the Act-BLM sample may be that binding of the OOH^- ligand induces disorder regardless of the presence of DNA substrate, either from a distribution of bonding orientations of the OOH^- itself or from the network of hydrogen bonds that is proposed to exist among the OOH^- ligand, the bleomycin macrocycle, and the DNA.[4g]

In the presence of DNA substrates, weakly hyperfine-coupled, nonexchangeable proton features occurred within 1 MHz of the free proton NMR frequency (see starred features of Figure S-4 of the Supporting Information). The resolution of these new features was best from Fe(III)-BLM, but new, 10-mer substrate-induced features were also observed near $^{H}\nu_{NMR}$ from Act-BLM. Protons with dipolar couplings ≤1 MHz will be ≥4.5 Å from the metal. At present it is not clear to us if these are protons of the BLM macrocycle whose distances from the iron were altered by DNA substrate binding or are protons of the DNA substrate itself; selective isotopic labeling of BLM and substrate oligonucleotides, especially at the nearby, chemically reactive 4′-hydrogen of cytosine, could resolve this question of assignment.

Conclusions

The discovery of ^{31}P hyperfine couplings provides a well-defined distance of 7.4 Å from iron of both Fe(III)-BLM and Act-BLM to DNA phosphate(s). ENDOR provided evidence that binding of Fe(III)-BLM to DNA substrate perturbs the protons of the BLM macrocycle, even though the hyperfine couplings to the immediate iron ligands were unchanged. There is the potential for resolving weaker interactions with more distant protons, possibly on the DNA substrate.

Acknowledgment. This research was supported in part by NIH Grant No. GM 35103 (C.P.S.). We are grateful to Professor B. M. Hoffman for providing us his GENDOR simulation routine for angle-selected ENDOR and to Professor S. M. Hecht for providing coordinates of the Zn-BLM−d(CGCTAGCG)$_2$ complex.

Supporting Information Available: Figure S-1, comparing computed ^{31}P angle-selected ENDOR spectra with experimental ^{31}P spectra from Fe(III)-BLM in the presence of 10-mer substrate, Figure S-2, comparing the exchangeable proton features previously assigned (ref 5a) to axial exchangeable protons of Fe(III)-BLM in the presence and absence of 10-mer substrate, Figure S-3, showing ^{14}N and ^{17}O hyperfine couplings from Act-BLM and Fe(III)-BLM in the presence and absence of 10-mer substrate, and Figure S-4, comparing proton ENDOR spectra of weakly coupled nonexchangeable protons within ±0.5 MHz of $^{H}\nu_{NMR}$ for Fe(III)-BLM and for Act-BLM in the presence and absence of 10-mer substrate (5 pages). See any current masthead page for ordering and Internet access instructions.

JA972138W